Title: Understanding the EROS2 Observations Towards the Spiral Arms Within a Classical Galactic Model Framework

Date: Oct 04, 2011 11:00 AM

URL: http://pirsa.org/11100080

Abstract: I will introduce the gravitational microlensing, its application to the compact dark matter detection and the extra-solar planet observations. EROS has been performed the microlensing observation in four directions of the Galactic plane, away from the Galactic center. I will report the observational results and the interpret the data within the Standard Galactic model. As a result we extract the best fit to the dust contribution in the Galactic disk, orientation of the Galactic bar and the abundance of the red giants compare to local stellar distribution.

Interpretation of EROS gravitational microlensing data towards Spiral Arms

Sohrab Rahvar

Sharif Univ of Tech.

Collaborators: M. Moniez, R. Ansari and O. Perdereau (CNRS-LAL)

Gravitational Lensing

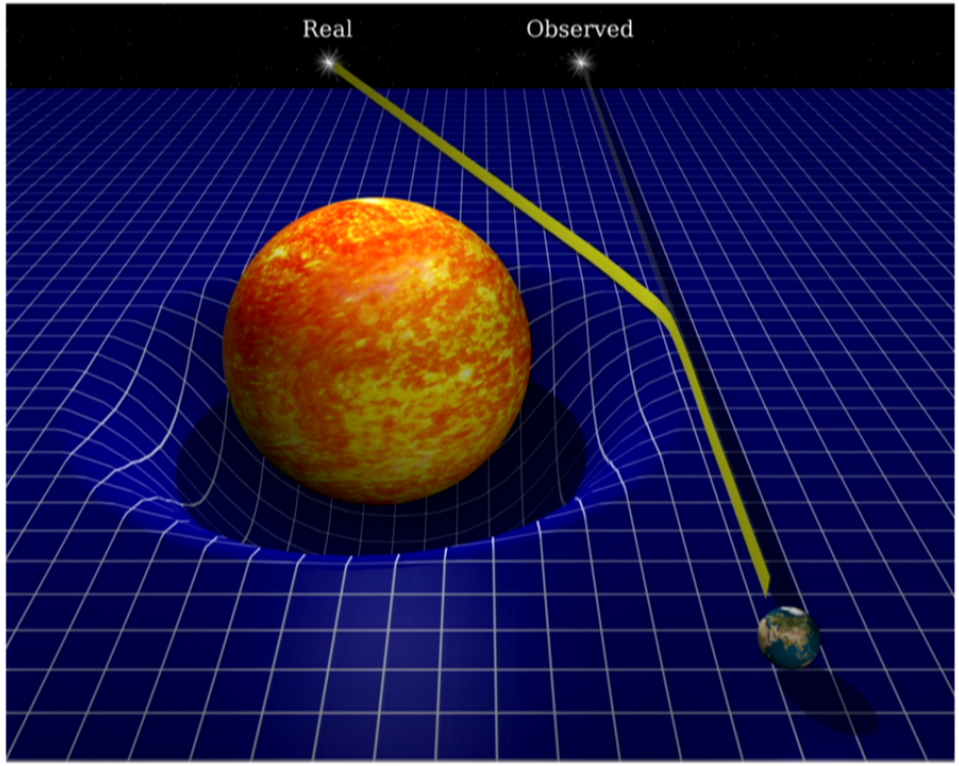

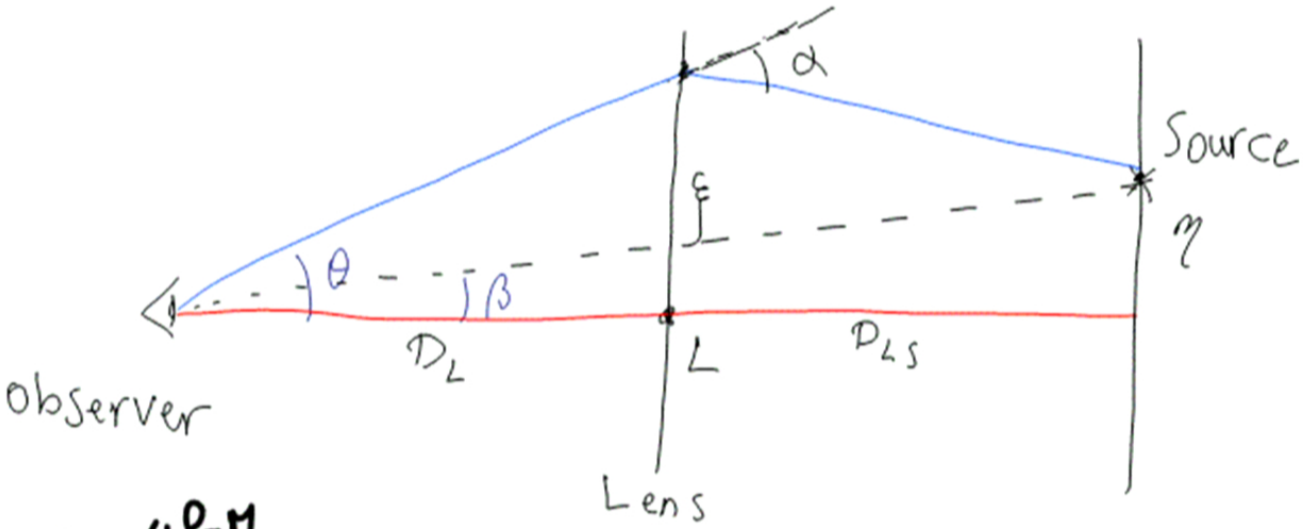

$$\alpha = \frac{4GM}{c^2 \xi}$$

$$\Phi(\theta;\beta) = \Delta t_{ge} + \Delta t_{gr}$$ Fermat potential

$$\phi(\theta;\beta) = \frac{1}{2}(\theta-\beta)^2 + \Psi(\theta;\beta), \quad \Psi = \theta_E^2 \ln \theta/\theta_0$$

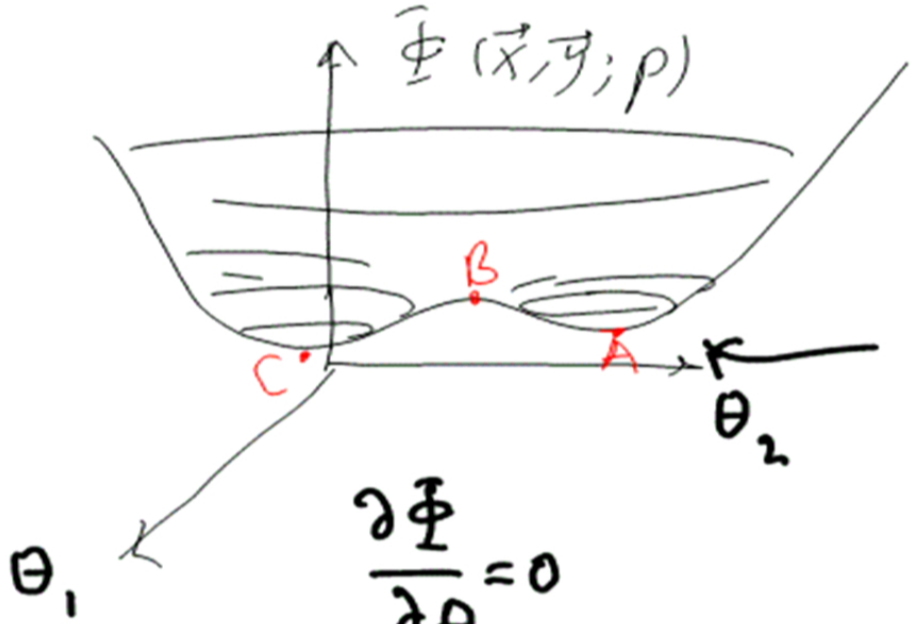

$$\frac{\partial \Phi}{\partial \theta} = 0$$

$$\theta - \beta + \psi_{,\theta} = 0 \longrightarrow \frac{\partial \beta}{\partial \theta} = \delta_{ij} + \psi_{,ij}$$

changing the light bundle : $J = \det \left| \frac{\partial \beta}{\partial \theta} \right|$

Light Magnification $A = 1/J$

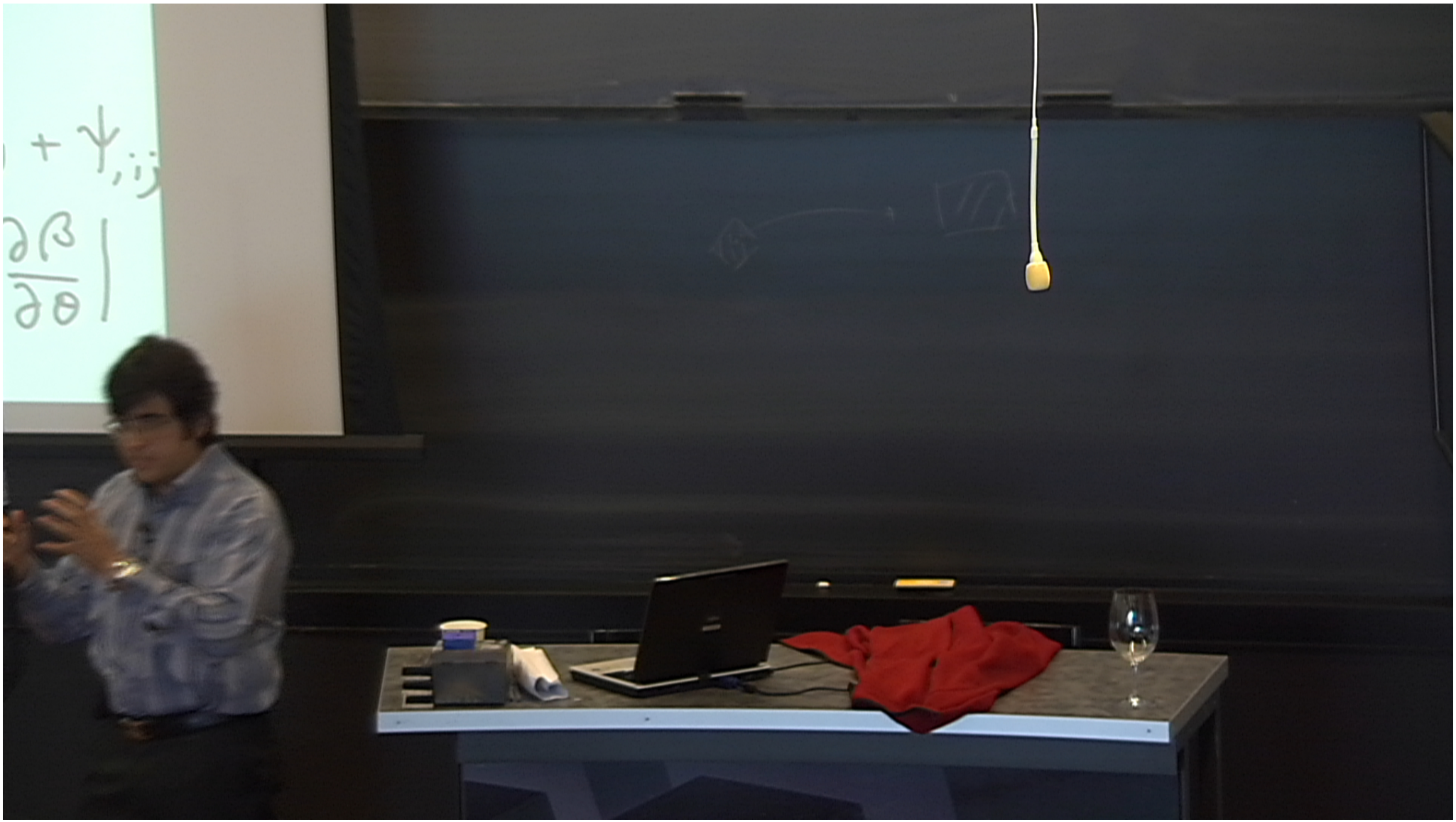

Credits: Lenses - David Cochrane

Gravitational Lensing in Large Scale

star-star lensing inside of Milky Way

- Unlike to the Cosmological scales where observer-lens and source do not change in our life time, in the Galactic scales all these elements changes by time in the order of one month
- Problem with this lensing is that angular separation between the images are in the order of mille arcsec (Micro-Lensing) , below the angular separation of ground base telescopes
- The probability is very low, about one event per one million star

star-star lensing inside of Milky Way

- Unlike to the Cosmological scales where observer-lens and source do not change in our life time, in the Galactic scales all these elements changes by time in the order of one month
- Problem with this lensing is that angular separation between the images are in the order of mille arcsec (Micro-Lensing) , below the angular separation of ground base telescopes
- The probability is very low, about one event per one million star

A brief history

1. Einstein (1936): “there is no great chance of observing this phenomenon’.
2. Paczynski (1986): Suggested microlensing of observation of Massive Astrophysical Compact Halo Objects (MACHOs) in the Galactic halo
3. MACHO Collaboration (1993): First observation of Microlensing
4. Several groups as EROS, MACHO, OGLE, MOA, …. Started monitoring of Spiral arms, bulge, LMC & SMC and even M31 for observing microlensing
5. In recent years microlensing is used as a technique for extra-solar planet detections

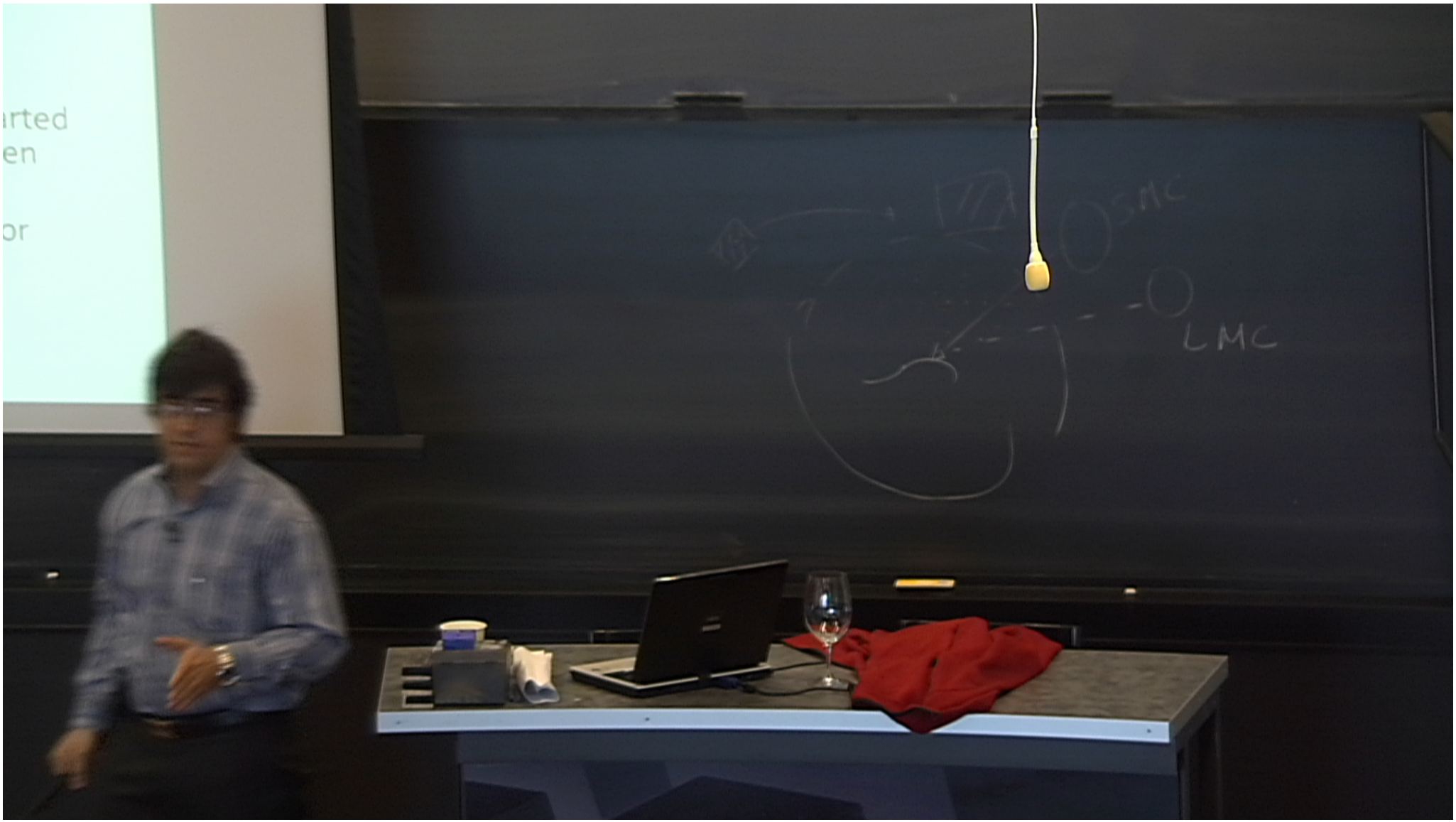
arted
en
or
SMC
LMC

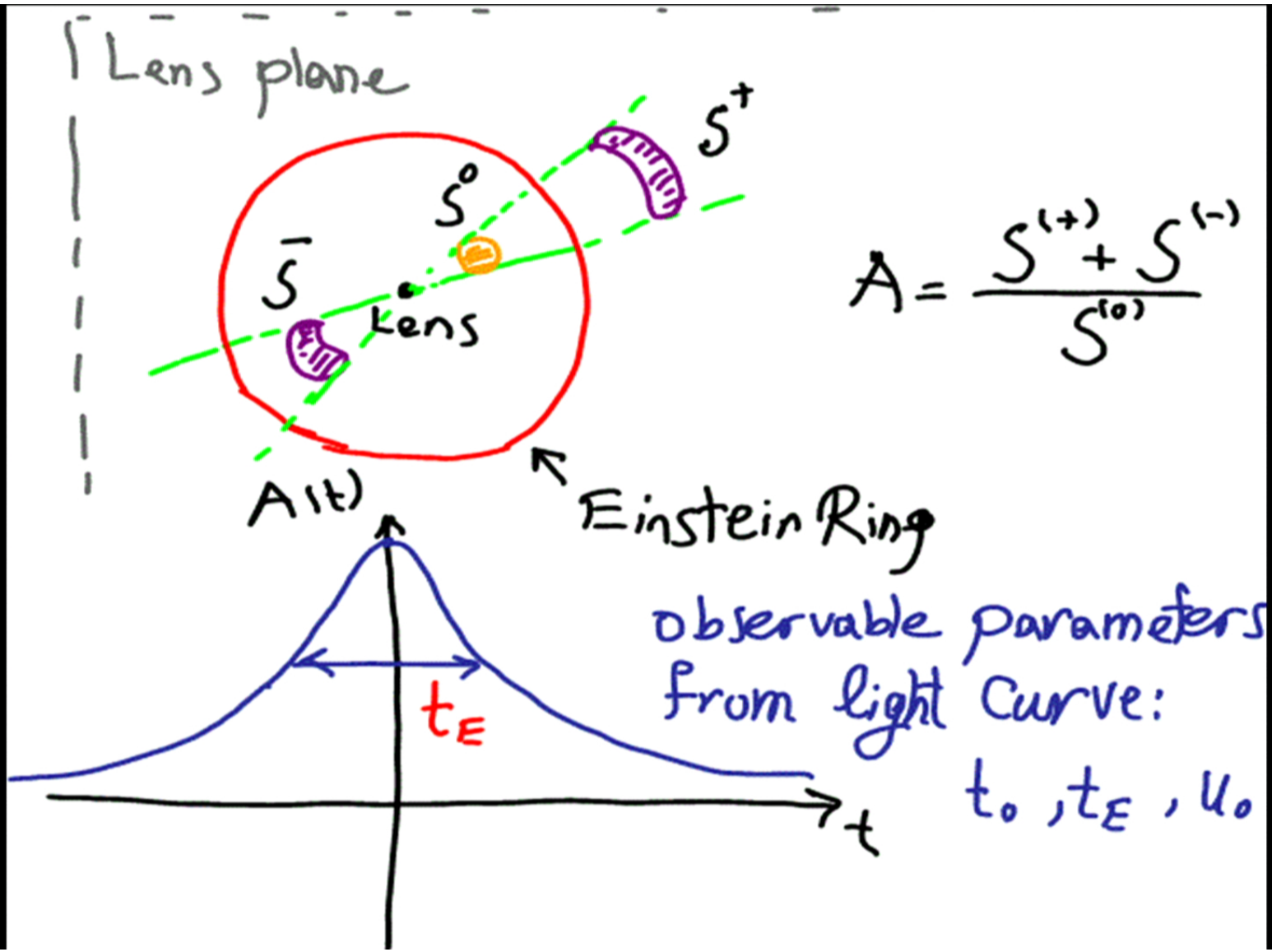

$$A = \frac{S^{(+)} + S^{(-)}}{S^{(0)}}$$

observable parameters from light curve:

t_0, t_E, u_0

probability detection (optical depth)

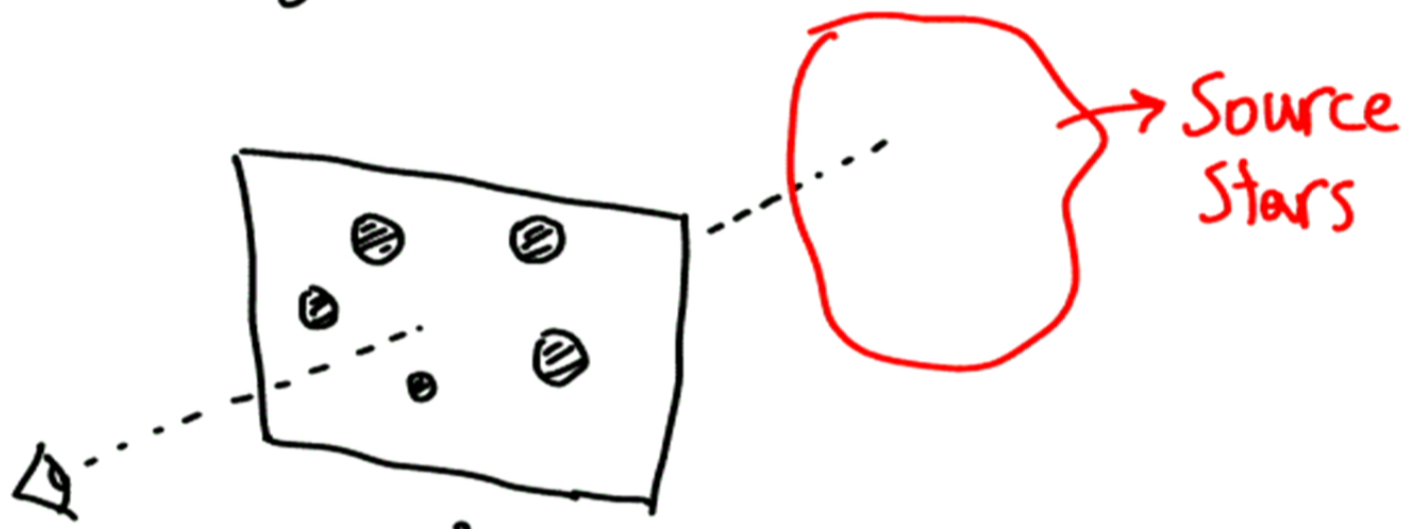

$$d\tau = \frac{\delta(\sum \pi R_E^2)}{A} = \frac{1}{A}\frac{\rho(x)}{m} A\,dx \cdot \frac{4\pi G}{c^2} m D$$

$$\tau = \int \rho(x) \cdot \frac{4\pi G}{c^2} D\,dx \simeq G D^2 \rho = \frac{M}{D}\frac{G}{c^2}$$

$$\tau = \frac{GM}{Dc^2} \simeq \left(\frac{v}{c}\right)^2 \simeq 10^{-6}$$

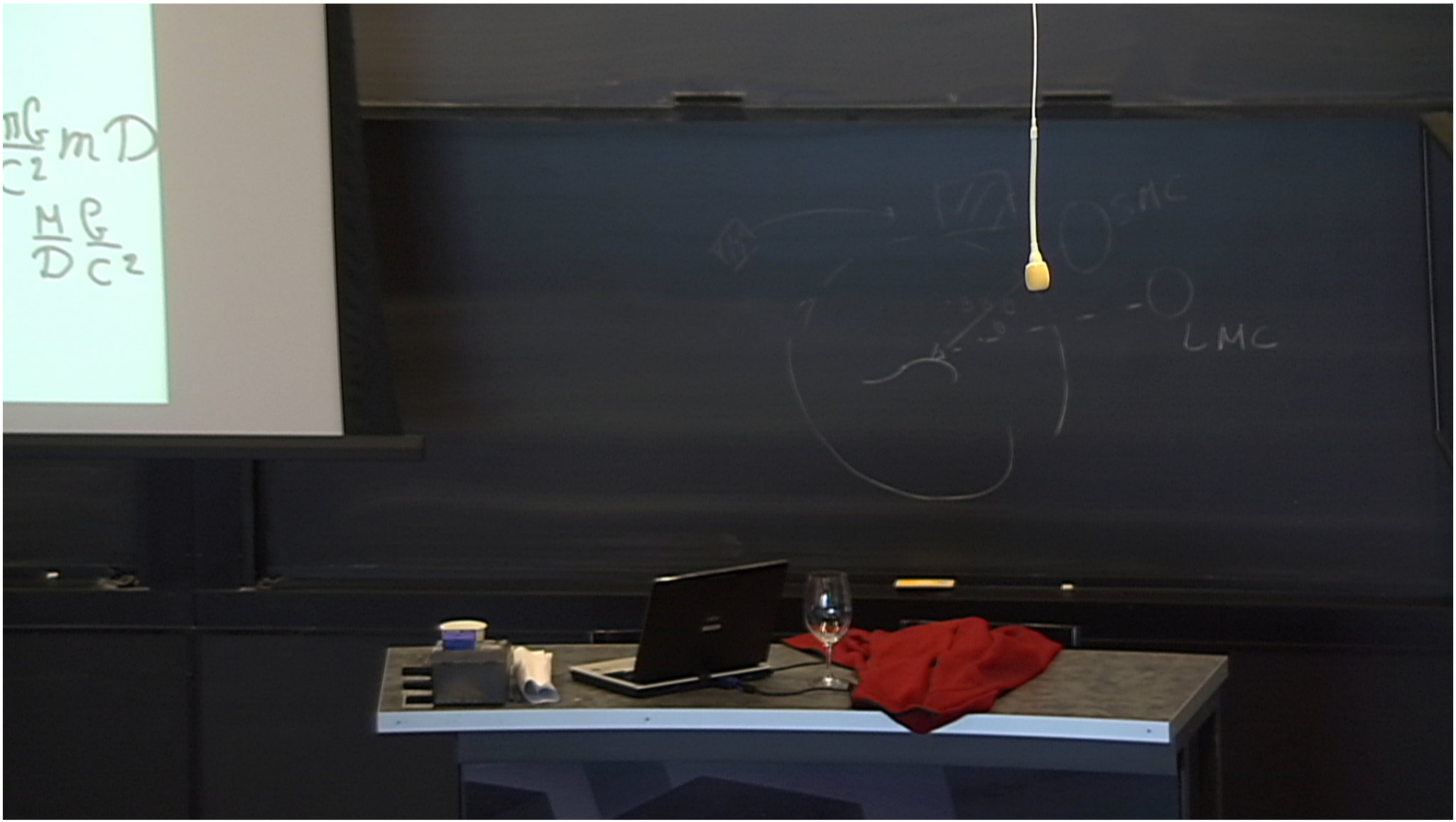
SMC
LMC

In observation

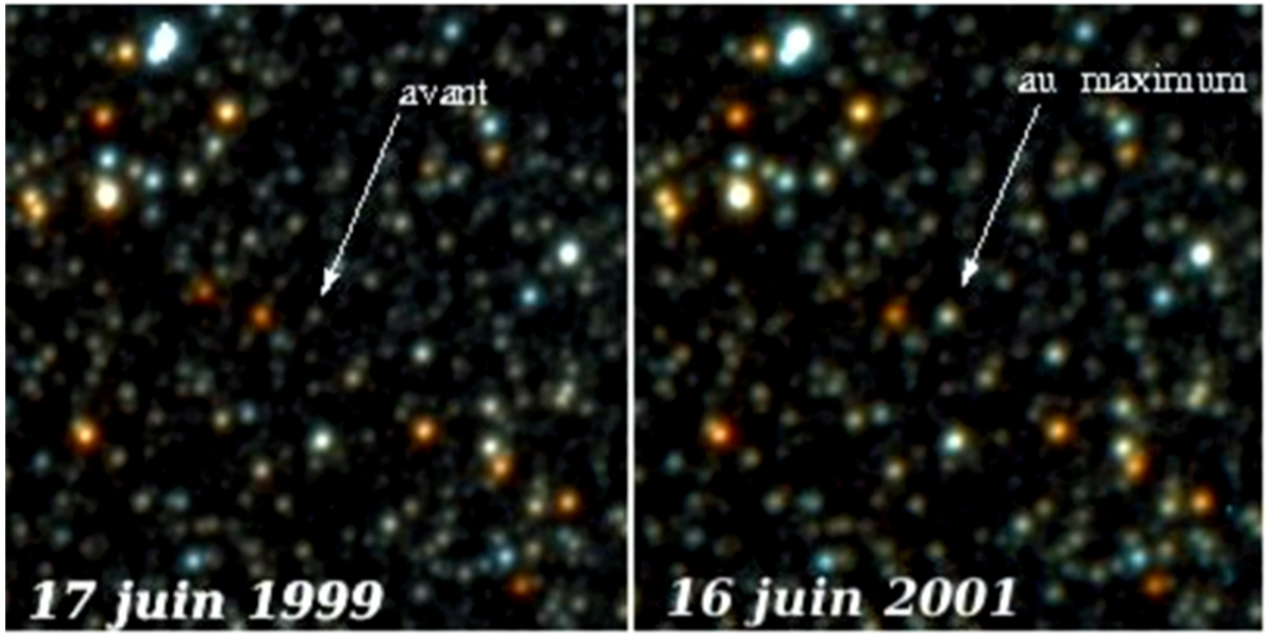

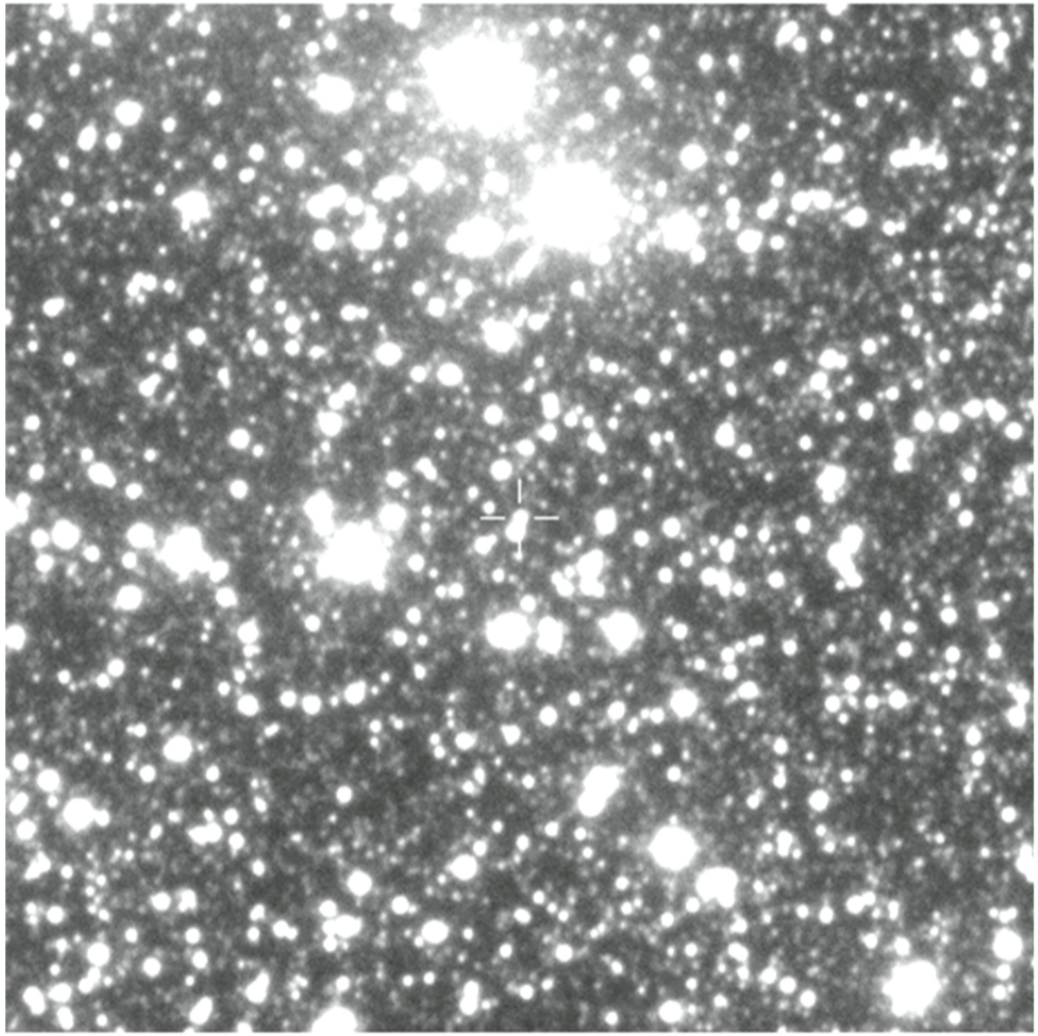

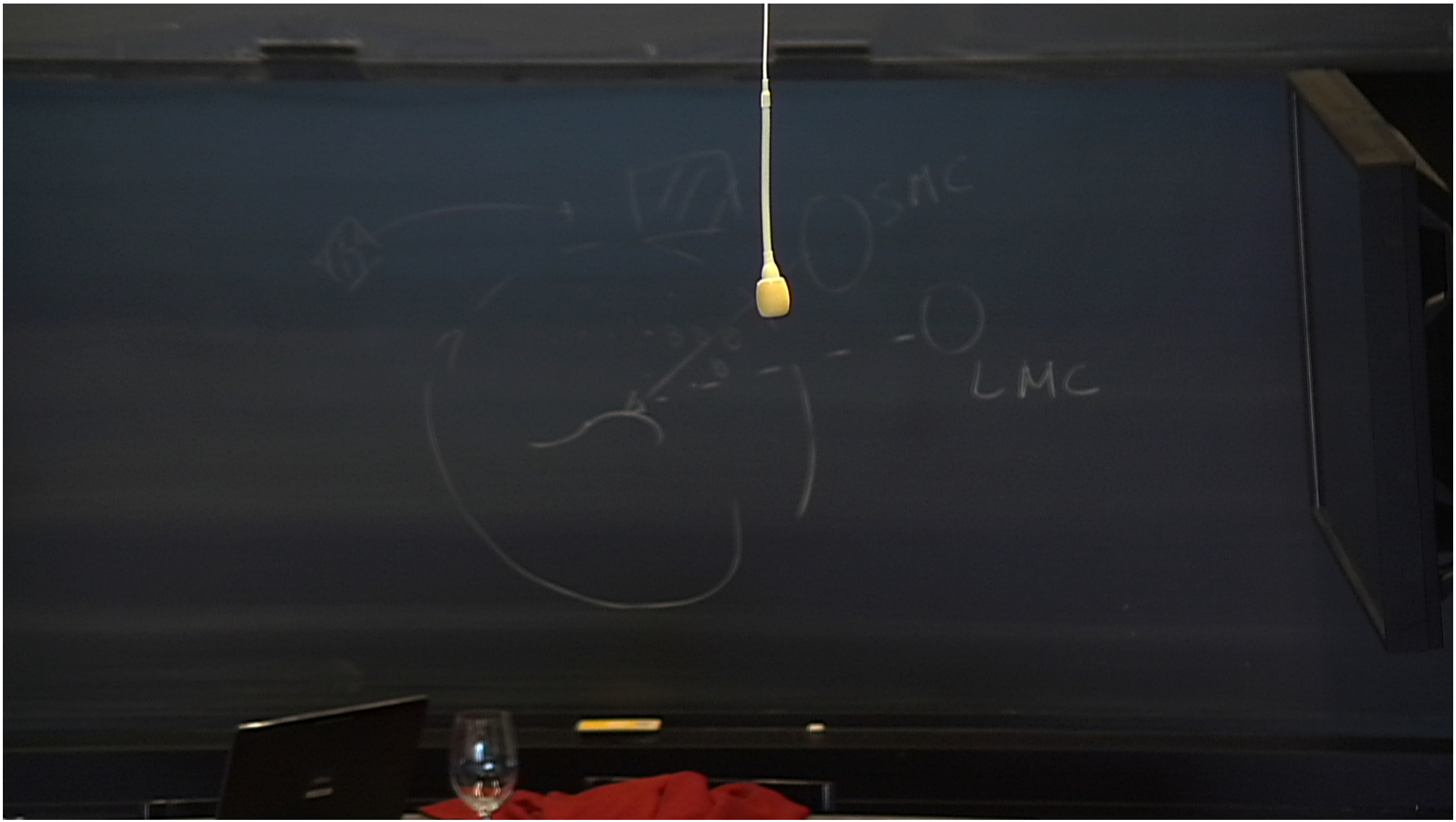
SMC
LMC

First Microlensing Event

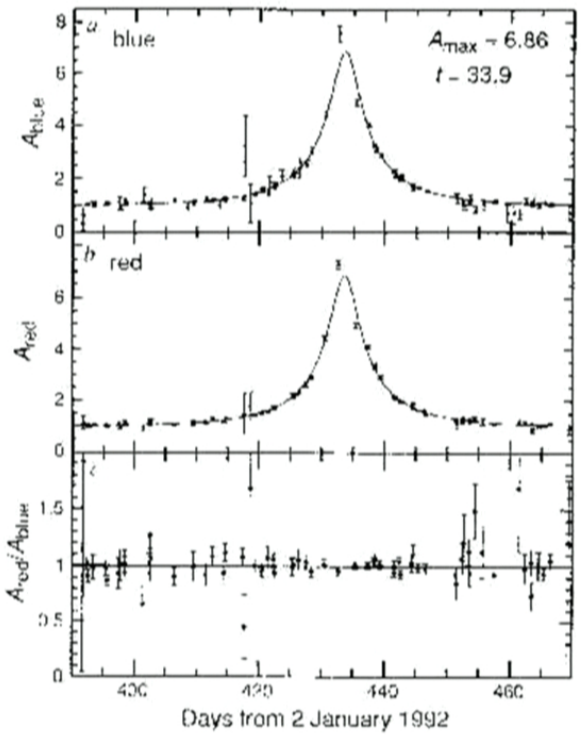

Alcock et a. Nature (1993)

EROS, MACHO and OGLE observations for searching Galactic MACHOs

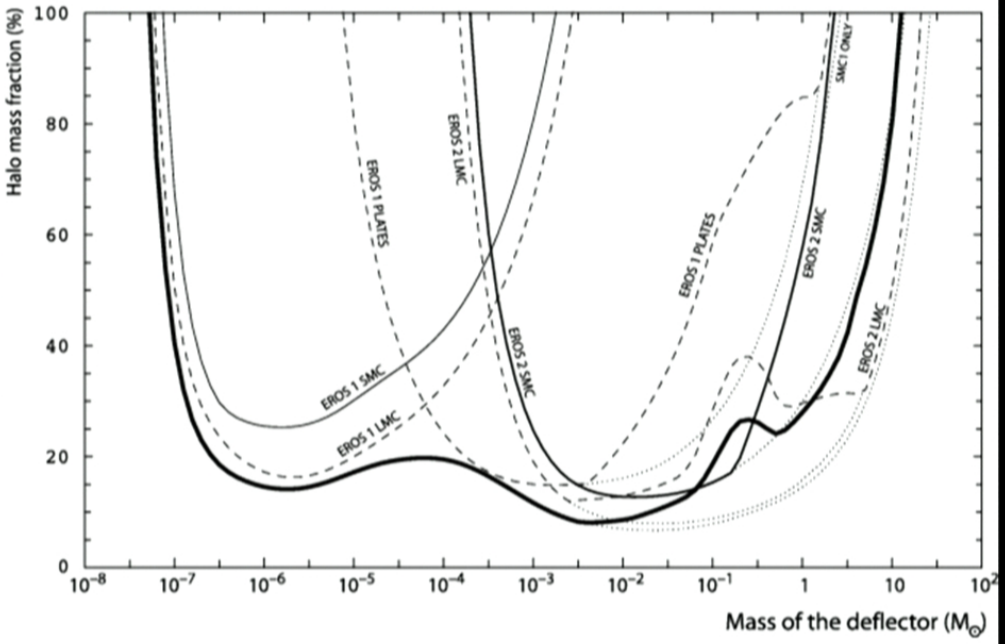

Afonso et al. (EROS) A&A 400, 951-956 (2003)

There is not enough MACHOs in the Galactic Halo

Next Application of gravitational Microlensing in extra-solar planet detection

For the case there are two or more lens

In the linear regime we Can use Superposition of gravitational potential.

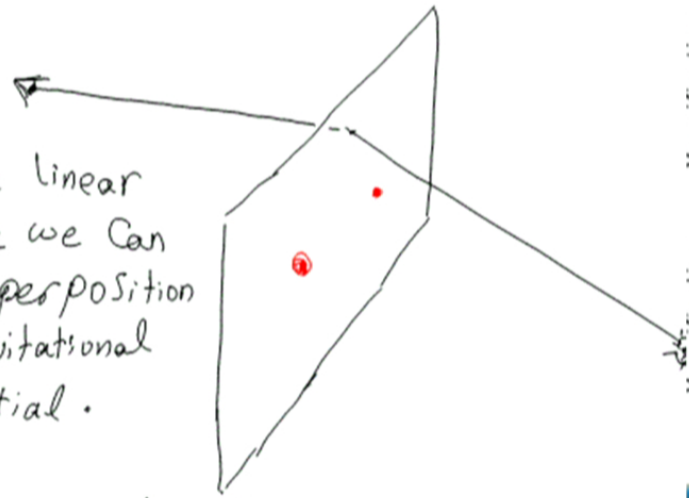

Lens plane

Lens plane

$$J = \det\left|\frac{\partial \beta}{\partial \theta}\right| = 0$$

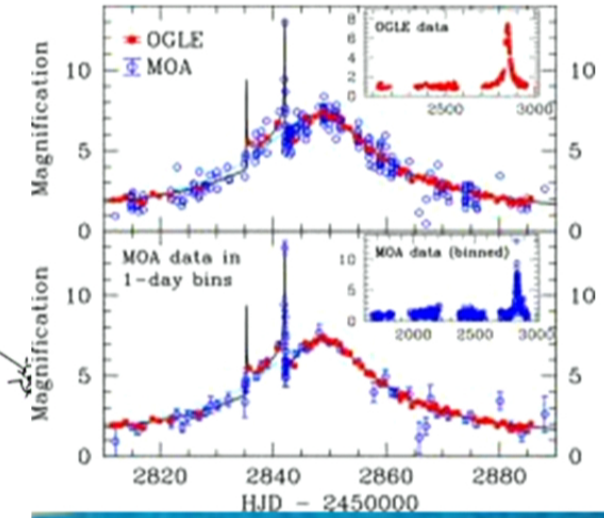

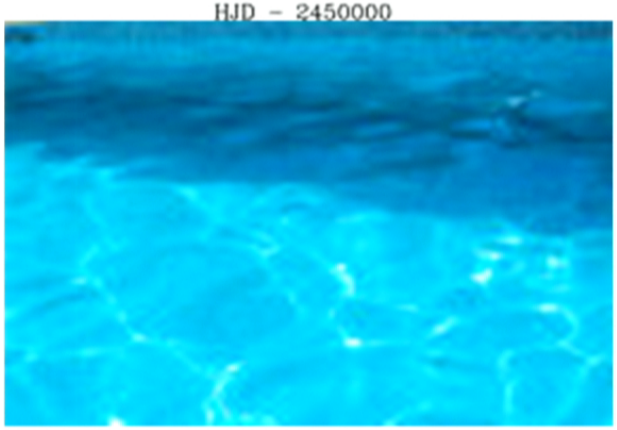

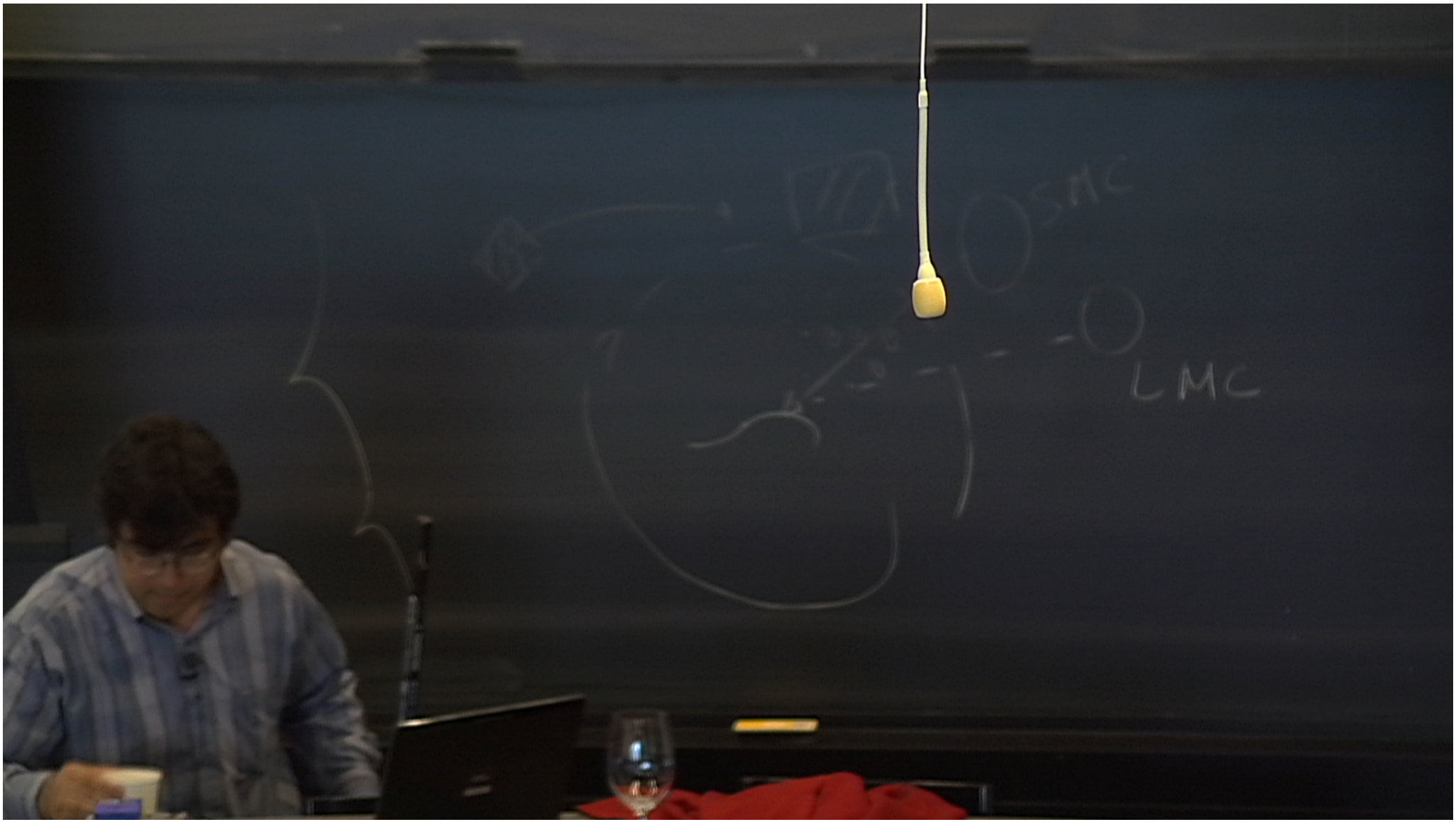
SMC
LMC

Caustics for binary lens with q=0.1

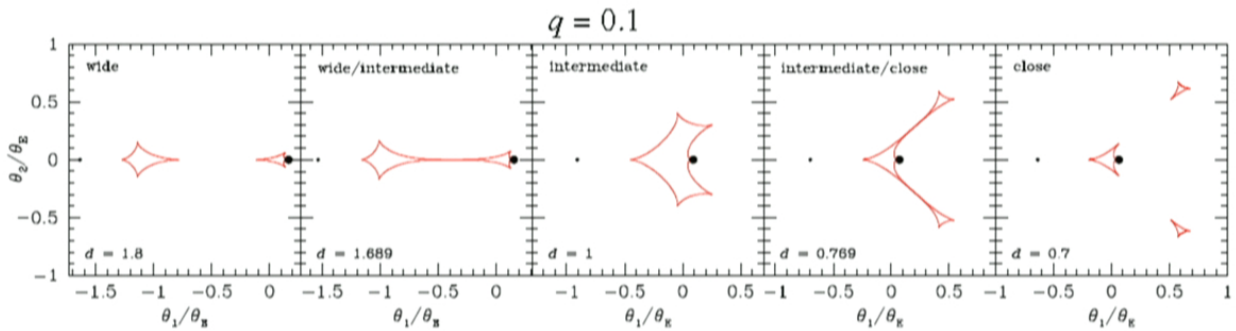

Martin Dominik GRG (2010)

Planet detection by Microlensing

- Mao and paczynski (1991) proposed detection of planet by this method:

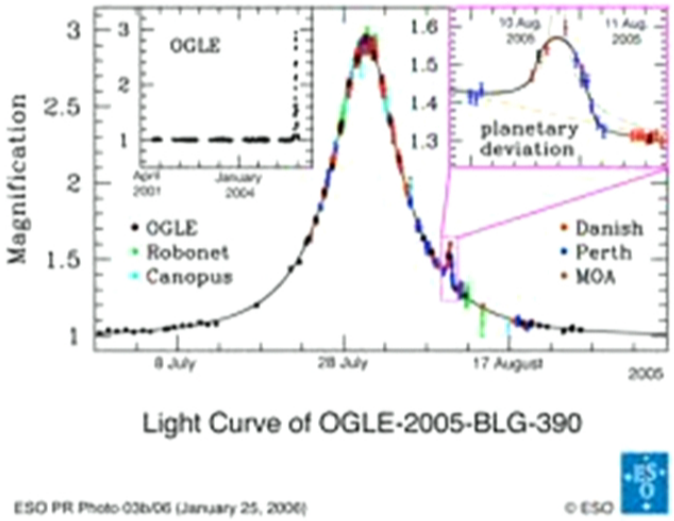

Light Curve of OGLE-2005-BLG-390

Advantage of the Microlensing is that we can detect planets beyond the snowline
Gould et al (2010) ApJ

MOA-2009-BLG-319Lb

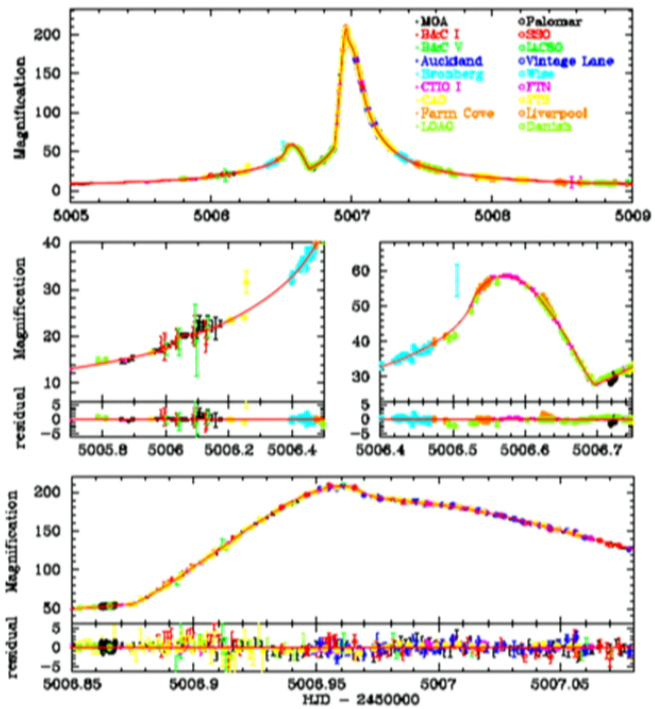

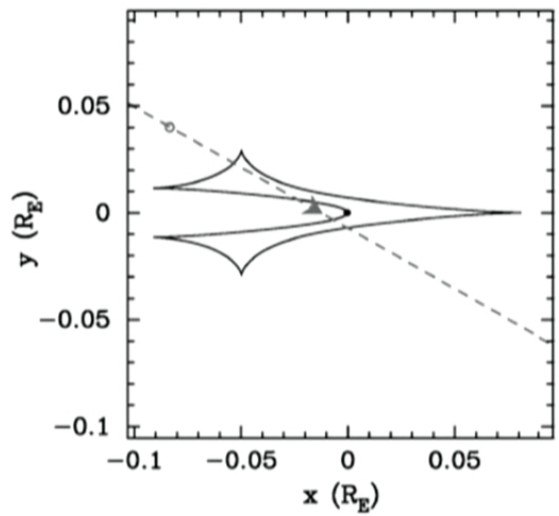

The advantage of the exoplanet microlensing observation is that we can observe distant planets beyond the snow line. Which is not the case for the transit or Doppler methods

EROS observation towards Spiral Arms

- Marly 1 meter

EROS-1 *(1990-1995)*

EROS-2 *(1996-2003)*

Observational Fields in the Spiral Arms

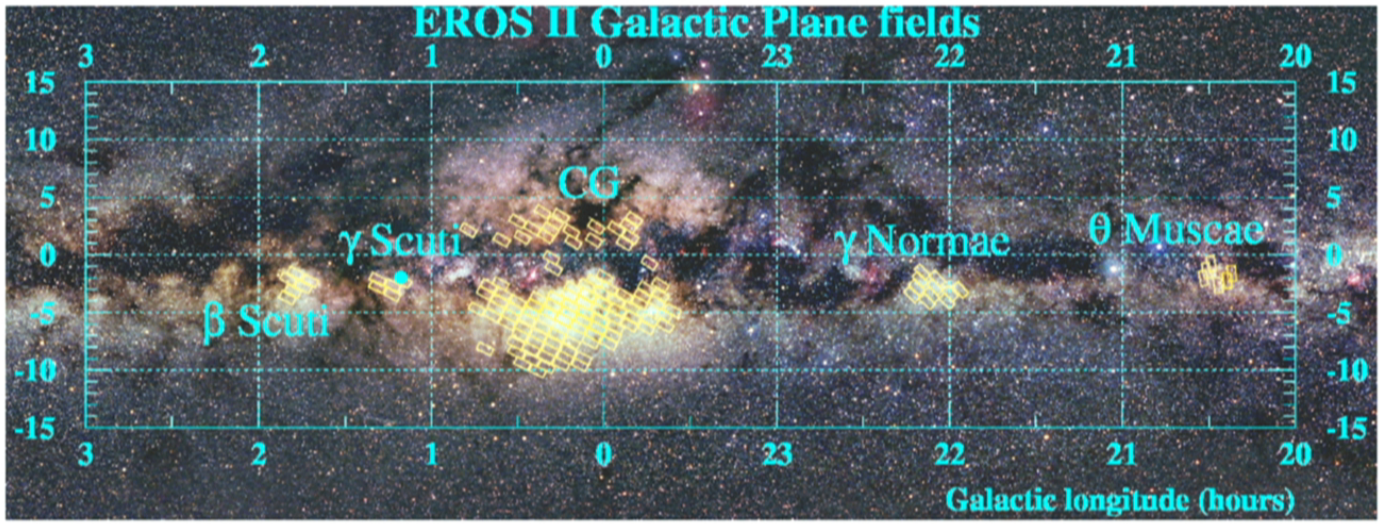

Rahal et al (EROS coll.) A&A (2009)

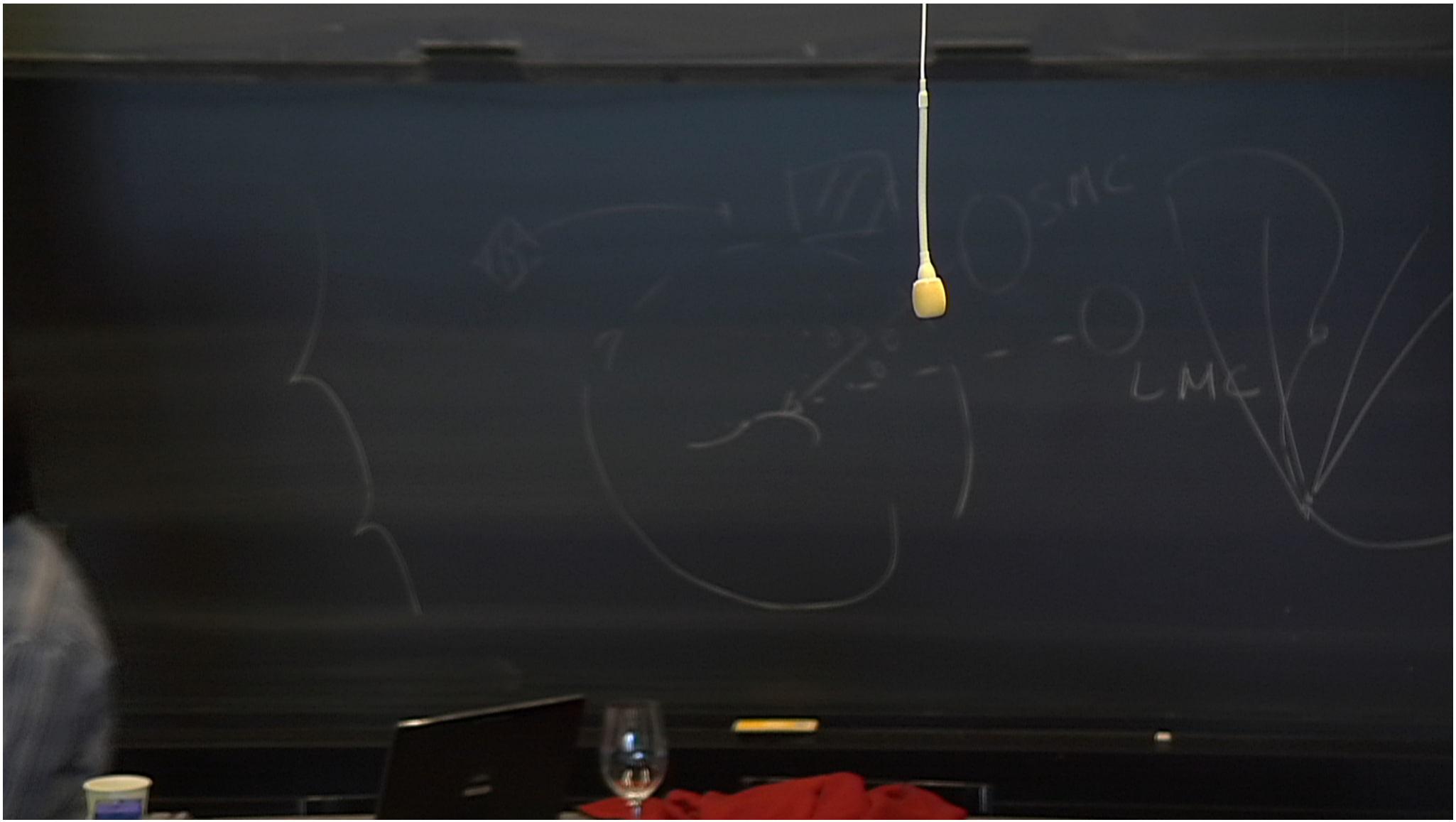
OSMC
LMC

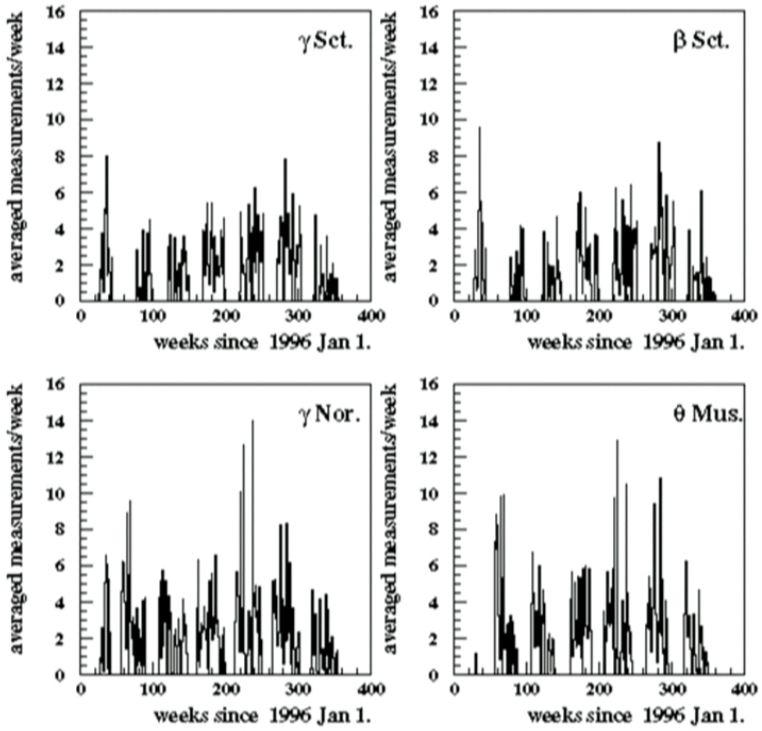

Field	α°, δ° ($J2000$)	b°	l°	N_{meas}	N_{obs} (10^6)
β Sct **Exposure** = **120 s. f.o.v. = 4.3** deg^2.				268	3.00
γ Sct **Exposure** = **120 s. f.o.v. = 3.6** deg^2.				277	2.38
γ Nor **Exposure** = **120 s. f.o.v. = 8.4 deg^2**.				454	5.24
θ Mus **Exposure** = **180 s. f.o.v. = 3.8** deg^2.				375	2.28

22 Microlensing event observed from the seven season observation 1996-2003

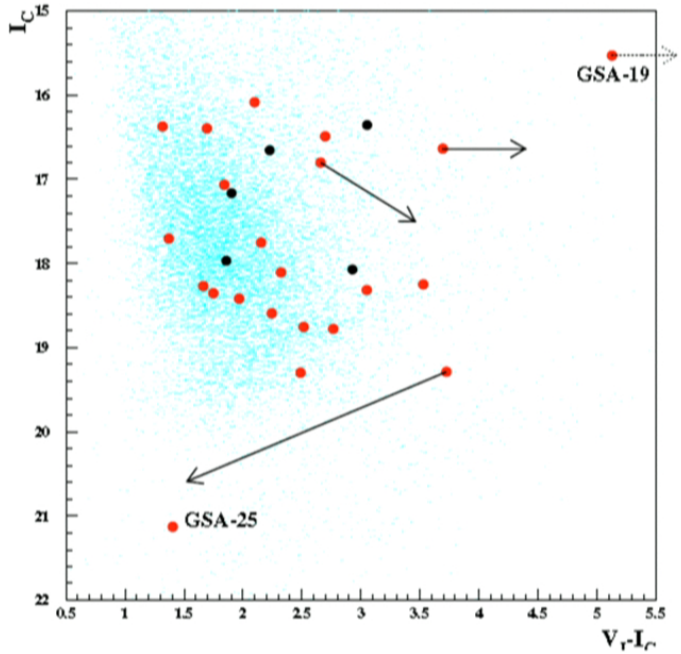

	θ Mus	γ Nor	γ Sct	β Sct	
$b°$	−1.46	−2.42	−2.09	−2.15	
$l°$	306.56	331.09	18.51	26.60	
		Observations			**All**
$\tau \times 10^6$	$.67^{+.63}_{-.52}$	$.49^{+.21}_{-.18}$	$.72^{+.41}_{-.28}$	$.30^{+.23}_{-.20}$	$.51^{+.13}_{-.13}$
N_{events}	3	10	6	3	22
$\bar{t}_E$ (days)	97 ± 47	57 ± 10	47 ± 6	59 ± 6	60 ± 9

22 Microlensing event observed from the seven season observation 1996-2003

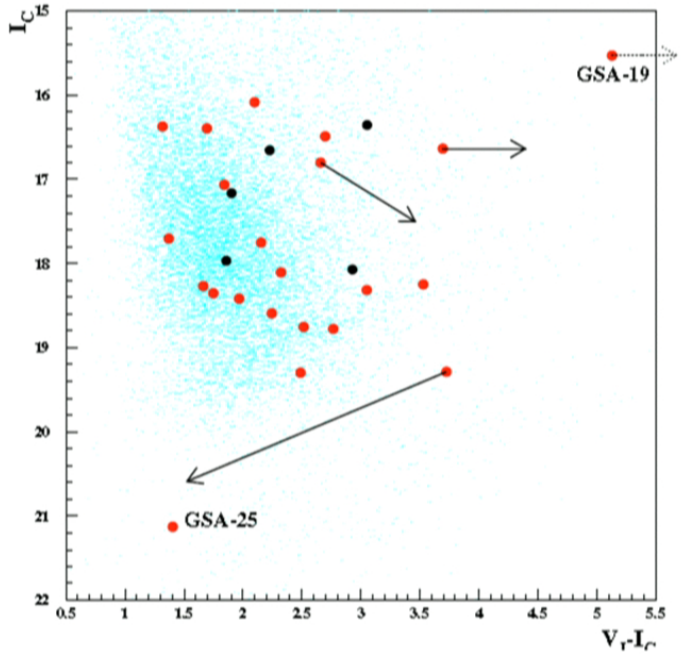

	θ Mus	γ Nor	γ Sct	β Sct	
$b°$	−1.46	−2.42	−2.09	−2.15	
$l°$	306.56	331.09	18.51	26.60	
		Observations			**All**
$\tau \times 10^6$	$.67^{+.63}_{-.52}$	$.49^{+.21}_{-.18}$	$.72^{+.41}_{-.28}$	$.30^{+.23}_{-.20}$	$.51^{+.13}_{-.13}$
N_{events}	3	10	6	3	22
$\bar{t}_E$ (days)	97 ± 47	57 ± 10	47 ± 6	59 ± 6	60 ± 9

Candidate	Field	α°, δ° (J2000)		I_C ($V_I - I_C$)	t_0 (days)	t_E (days)	u_0	χ^2/d.o.f	$\tau(10^{-6})$	Note
					γ Sct					
GSA1	200	277.2888	−14.2528	18.3 (3.1)	301.2 ± 0.1	64.0 ± 1.2	.043 ± .0010	299.7/435	0.146	
GSA8	200	276.8042	−15.0311	16.6 (3.7)	996.9 ± 0.1	40.6 ± 1.0	.145 ± .003	981./533	0.114	(1)
			Standard fit parameters:		993.0 ± 0.1	35.2 ± 0.7	.155 ± .002	1400./535		
GSA9	200	277.1750	−15.1644	18.8 (2.8)	1760.3 ± 1.7	57.9 ± 3.6	.482 ± .0158	262.9/565	0.142	
GSA10	200	277.2813	−14.8931	18.1 (2.3)	1806.1 ± 0.8	24.6 ± 1.3	.574 ± .0179	237.9/596	0.081	
GSA11	201	278.1650	−14.1094	18.8 (2.5)	1725.3 ± 0.4	44.3 ± 1.4	.187 ± .0049	367.2/558	0.116	
GSA12	203	278.5875	-13.9794	17.1 (1.8)	1378.6 ± 0.2	50.1 ± 0.7	.225 ± .0030	89.3/339	0.123	
GSA13	203	278.9404	−14.5803	17.2 (1.9)	313.9 ± 1.2	37.2 ± 2.1	.898 ± .0153	244.9/617	–	
GSA14	204	278.4388	−12.8678	16.7 (2.2)	1637.7 ± 3.4	68.4 ± 3.7	.785 ± .0097	421.2/392	–	(2)
					β Sct					
GSA15	301	281.0654	−6.0339	18.3 (3.5)	1399.8 ± 1.4	72.2 ± 2.8	.337 ± .0126	212.2/411	0.110	edge
GSA16	301	280.7646	−6.7583	16.4 (3.1)	1997.0 ± 3.2	60.6 ± 4.0	.796 ± .0141	341.8/361	–	
GSA17	302	281.3950	−7.8867	16.4 (1.7)	1947.2 ± 3.8	50.0 ± 2.4	.532 ± .1079	156.9/400	0.096	
GSA18	304	282.2879	−7.2500	16.1 (2.1)	1718.7 ± 0.1	55.0 ± 2.0	.137 ± .0009	133./514	0.098	(3)
			Standard fit parameters:		1718.4 ± 0.1	58.0 ± 0.3	.137 ± .0009	1556/516		
					γ Nor					
GSA2	400	242.9392	−52.9464	18.6 (2.3)	534.4 ± 0.2	98.3 ± 0.9	.342 ± .002	973.4/934	0.059	(4)
			Standard fit parameters:		533.6 ± 0.5	137.8 ± 2.6	.233 ± .0029	1196.5/937		
GSA19	401	244.1379	−52.0272	15.5 (5.1)	2367.7 ± 1.3	90.4 ± 3.0	.043± .025	893./880	0.063	(5)
			Standard fit parameters:		2373.5 ± 0.1	93.1 ± 0.7	.022 ± .007	1388.5/888		
GSA20	402	243.7758	−52.9700	16.4 (1.3)	2465.5 ± 1.0	40.± 5.0	.72 ± .02	414./696	0.039	(6)
			Standard fit parameters:		2487.1 ± 0.3	46.3 ± 0.7	.565± .0030	712.4/698		
GSA21	404	244.3063	−53.1100	16.8 (2.7)	1587.3 ± .03	74. ± 3.0	.0142 ± .0008	259./565	0.077	(7)
			Standard fit parameters:		1587.2 ± .03	39.1 ± 0.2	.037 ± .0007	1884.4/567		
GSA22	404	244.4263	−54.0508	18.4 (2.0)	2182.4 ± 0.2	26.6 ± 1.1	.048 ± .0180	429.5/742	0.031	
GSA23	404	245.1208	−53.9825	18.3 (1.7)	1573.8 ± 3.8	78.5 ± 5.7	.542 ± .0152	522.3/784	0.062	corner
GSA24	406	246.5442	−54.0394	18.0 (1.9)	2002.5 ± 1.4	55.5 ± 2.6	.720 ± .0158	579.4/786	–	
GSA25	408	247.6917	−53.9281	21.1 (1.4)	830.9 ± .03	67.6 ± 2.9	.003 ± .0001	876.2/771	0.037	(8)
GSA3	409	244.1129	−54.6303	17.7 (1.4)	696.0 ± 2.0	60.4 ± 3.0	.615 ± .0102	606.7/1090	0.051	
GSA26	411	241.8729	−55.3814	17.8 (2.2)	1642.1 ± 0.3	23.2 ± 0.8	.304 ± .0138	441.5/759	0.030	
GSA27	411	242.4846	−55.2292	18.3 (1.7)	2193.8 ± 0.1	6.8 ± 0.4	.210 ± .0068	433.6/831	0.022	
					θ Mus					
GSA28	501	202.2838	−64.2750	19.3 (3.7)	1992.2 ± 0.4	205. ± 20.0	.029 ± .004	717/499	0.431	(9)
			Standard fit parameters:		1992.0 ± 0.4	87.3 ± 3.0	.094 ± .0046	868.5/500		
GSA29	502	204.0683	−63.7117	19.3 (2.5)	1229.7 ± 0.3	74.2 ± 2.7	.082 ± .0042	161.7/354	0.166	
GSA30	505	199.2942	−64.2592	16.5 (2.7)	2396.9 ± 0.1	12.4 ± 0.2	.062 ± .0023	792.0/856	0.073	
					Uncertain candidate					
GSAu1	202	278.0371	−13.2851	18.1 (2.9)	1695.8 ± 6.9	409.3 ± 20.9	.708 ± .0155	426.9/613	–	

Measurable parameters:

- Rate of Events (Dynamics): $\Gamma = \frac{1}{N_{\rm obs}\Delta T_{\rm obs}} \times \sum_{\rm events} \frac{1}{\epsilon(t_{\rm E})}$
- Optical Depth(Static): $\tau = \frac{1}{N_{\rm obs}\Delta T_{\rm obs}} \frac{\pi}{2} \sum_{\rm events} \frac{t_{\rm E}}{\epsilon(t_{\rm E})}$
- Distribution of the Einstein crossing time
- Color Magnitude of the stars
- Average Number of Stars in the Field

Modeling Microlensing Events: Galactic Model

- Matter Distribution and dynamics of the stars in the Spiral arms and Bulge
- Stellar distribution in the Milky Way
- Mass function of the lenses
- Dust abundance

Galactic Model

Disk (double exponential):

$$\rho_D(r,z) = \frac{\Sigma}{2H} \exp\left(\frac{-(r-R_\odot)}{R}\right) \exp\left(\frac{-|z|}{H}\right)$$

σ_r (km s^{-1})	–	51.
σ_θ (km s^{-1})	–	38.
σ_z (km s^{-1})	–	35.

$V_{\mathrm{rot},\odot} = 220$ km s^{-1}

Bulge:

$$\rho_B = \frac{M_B}{6.57\pi abc} e^{-r^2/2}, \quad r^4 = \left[\left(\frac{x}{a}\right)^2 + \left(\frac{y}{b}\right)^2\right]^2 + \frac{z^4}{c^4}$$

$$f_T(v_T) = \frac{1}{\sigma^2_{\mathrm{bulge}}} v_T \exp\left(-\frac{v_T^2}{2\sigma^2_{\mathrm{bulge}}}\right),$$

with $\sigma_{\mathrm{bulge}} \sim 110$ km s^{-1}.

Extinction and reddening:

$$A(V)/N_H = 5.3 \times 10^{-22} cm^2$$
$$A(I)/N_H = 2.6 \times 10^{-22} cm^2$$

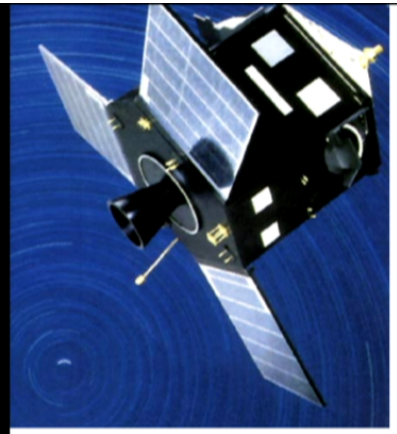

Stellar Model

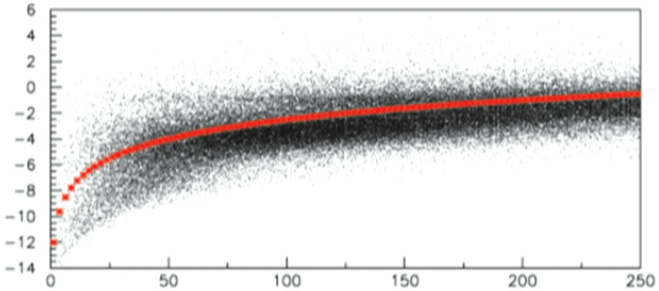

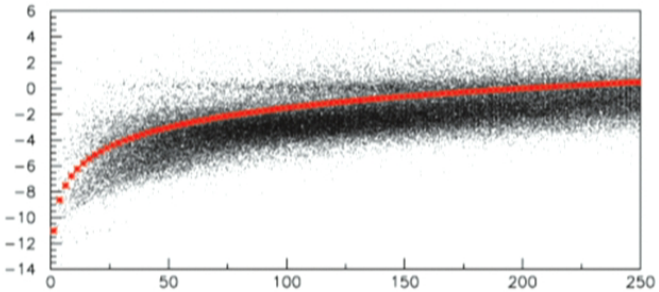

Using the Hipparcos data, we made a compelet sample. Hipparcos catalog has 118218 star and it is complete until the apparent visual magnitude of 7.5

Disk is almost homogenous up to 50 pc

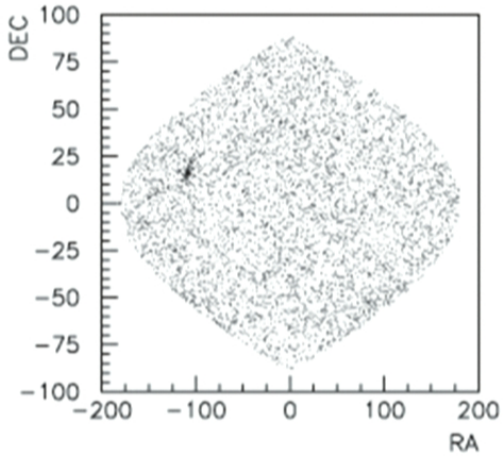

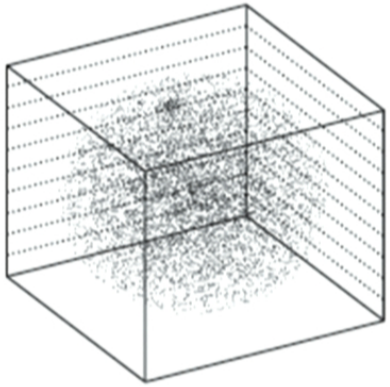

3D Distribution of stars

Starts in the complete Catalog of Hipparcos Data

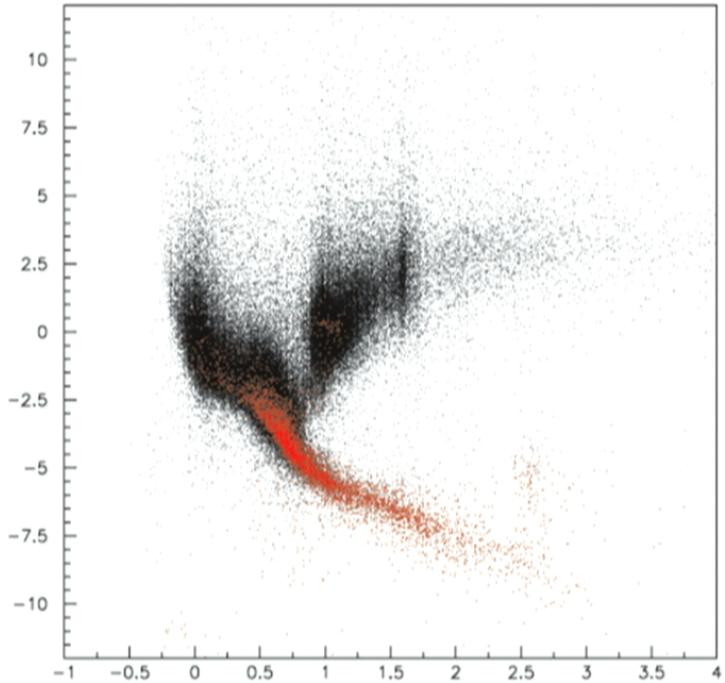

Hipparcos Catalog (solid) and complete sample (dashtes)

Unbiased distribution of the stars in color and magnitude

Observation in the direction of the Spiral arms

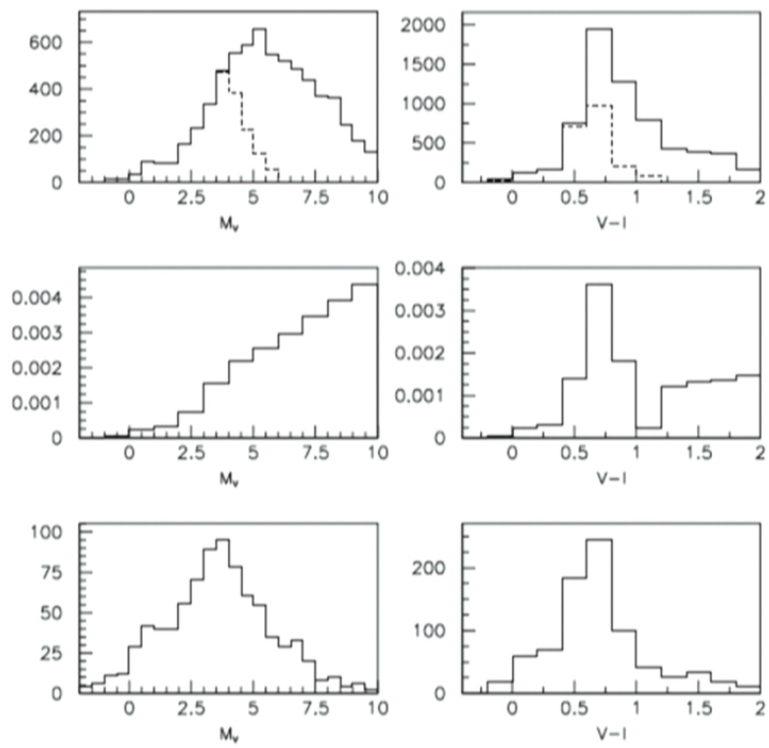

Generating EROS like catalog

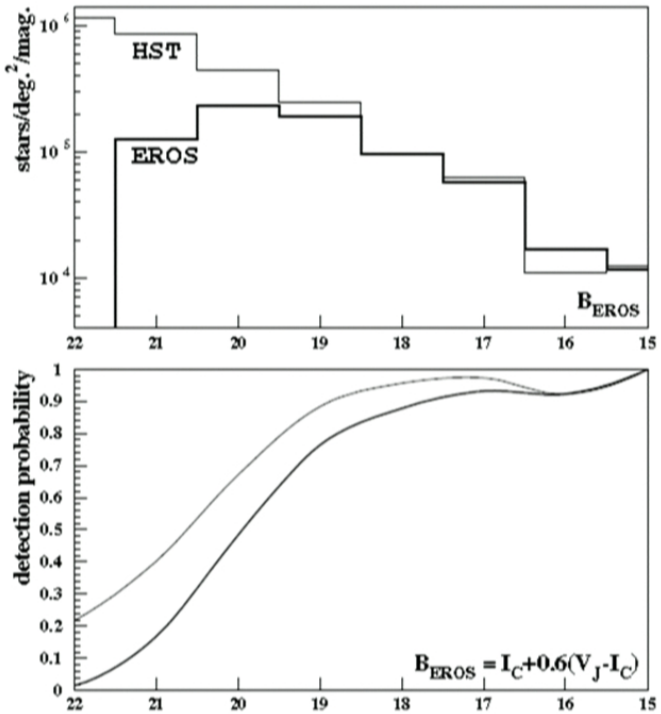

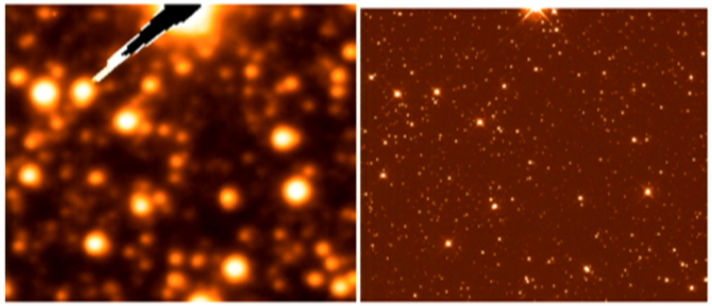

EROS vs. Hubble

synthesized CMD

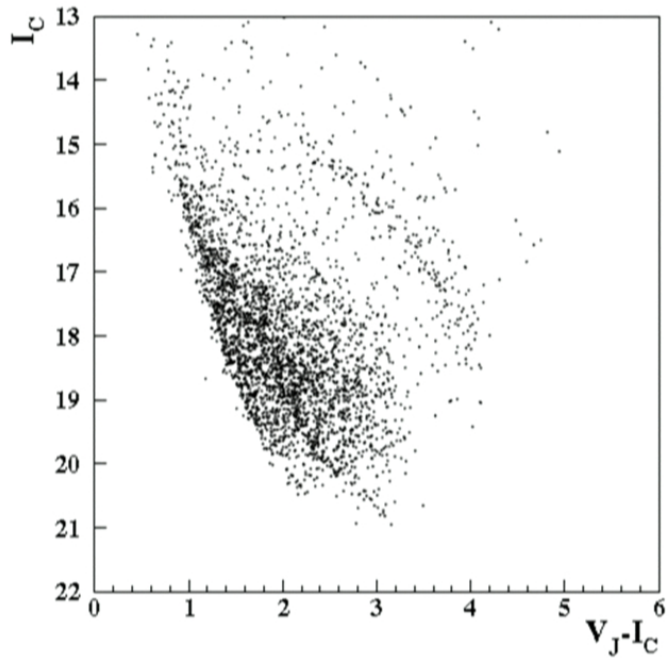

Fig. 21. Simulated color-magnitude diagram towards γ Sct (see text).

Compare with the observation

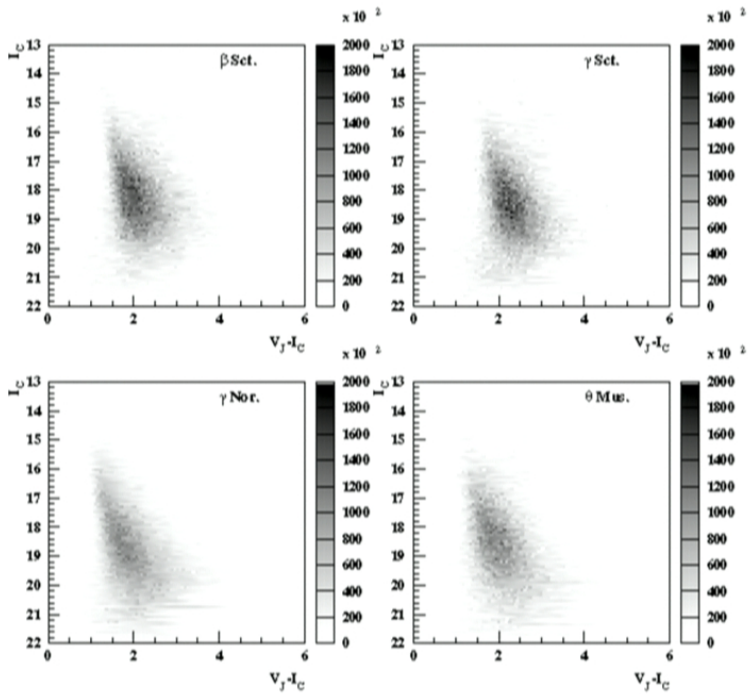

Compare with the observation

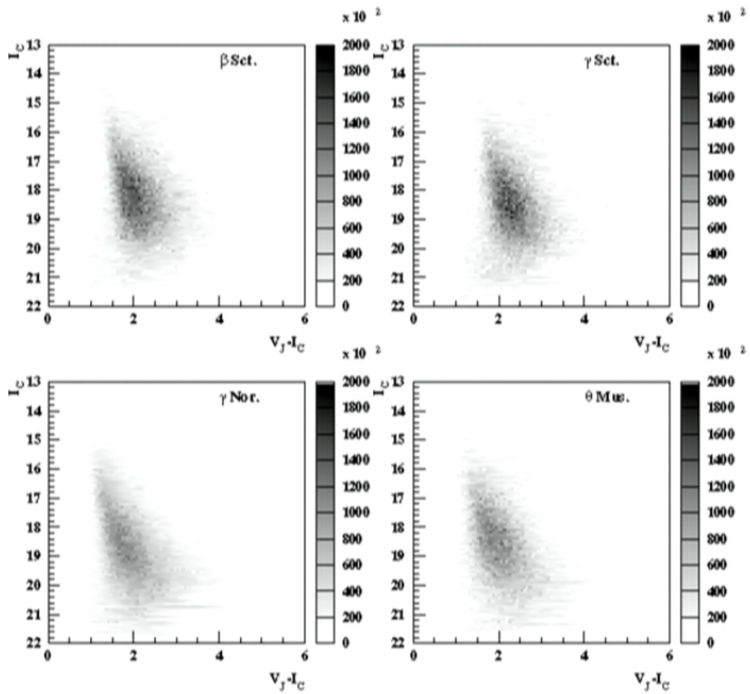

Compare with the observation

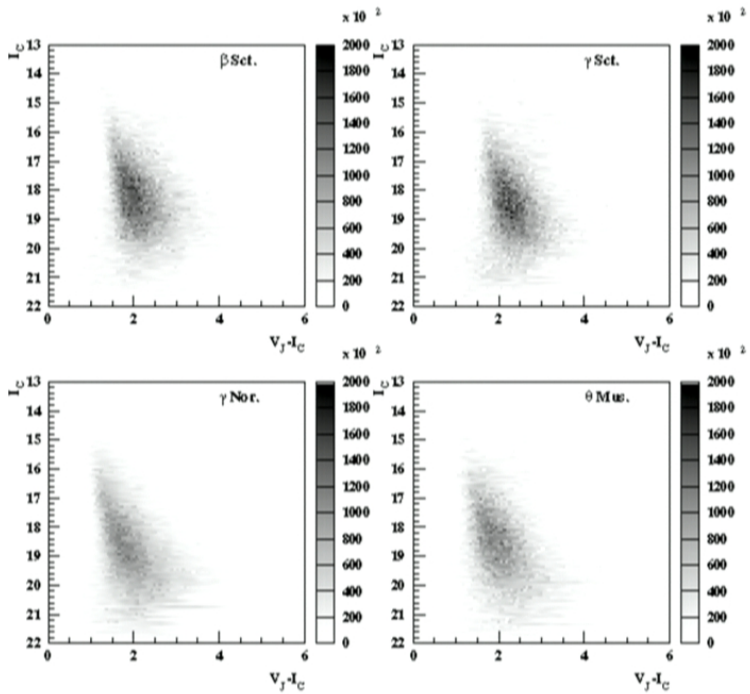

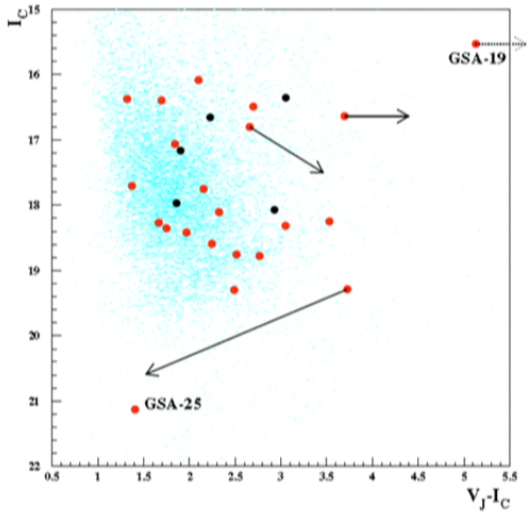

Microlensed stars are redder

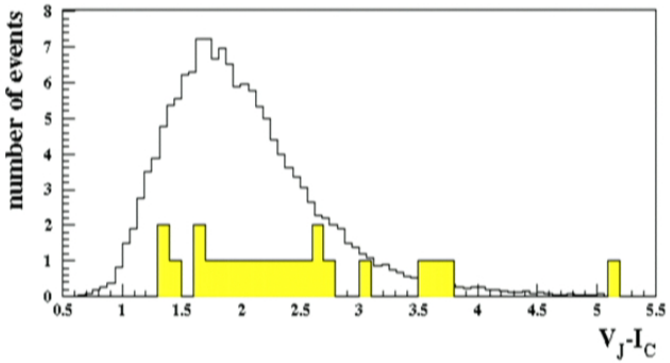

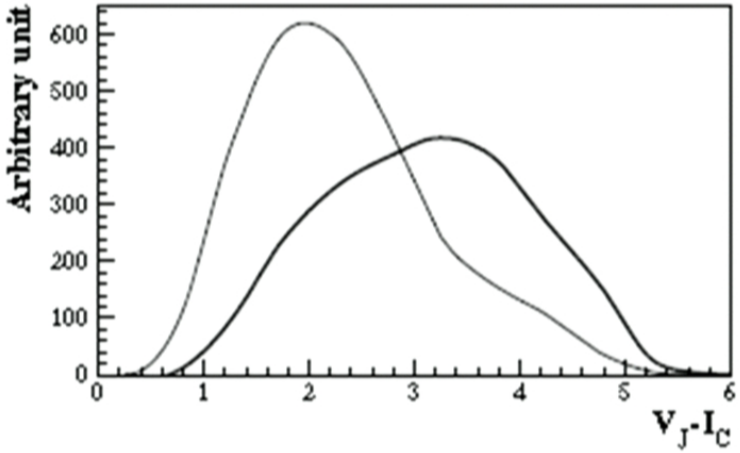

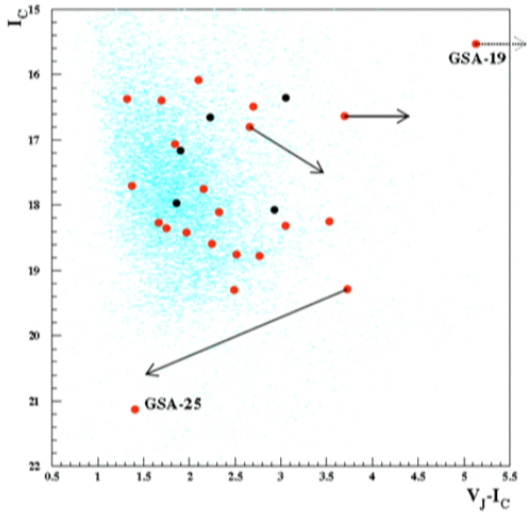

Microlensed stars are redder

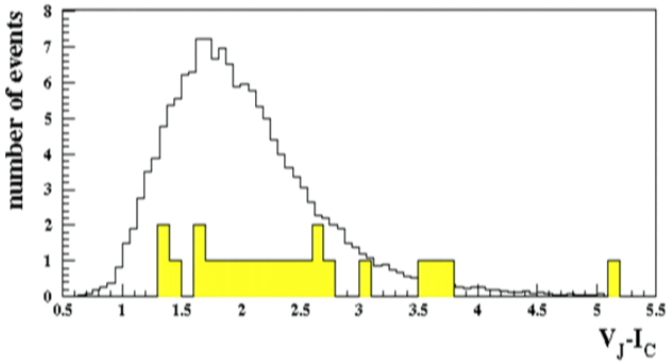

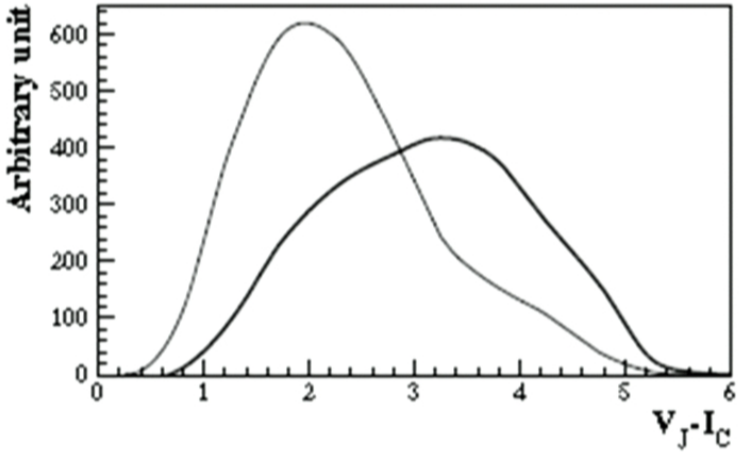

Optical Depth

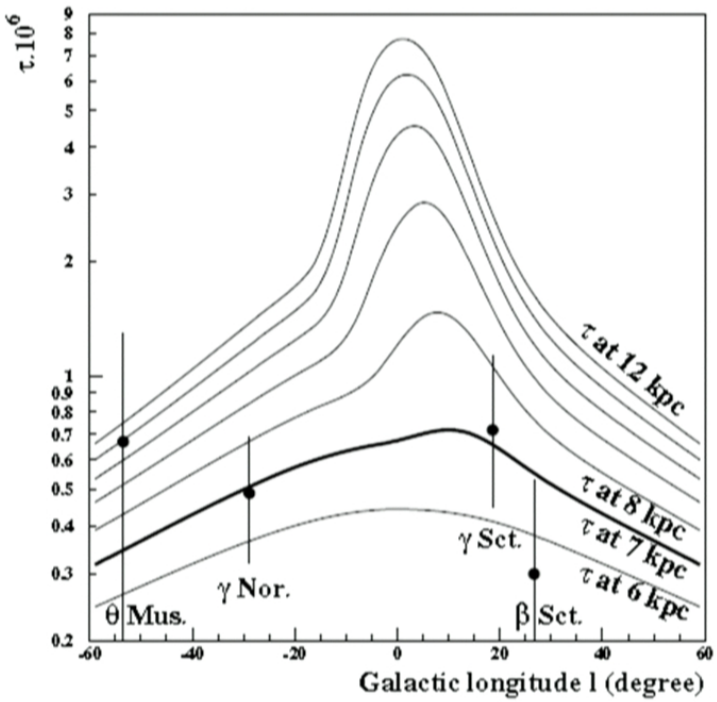

Preliminary results from paper, Rahal et al (2009)

Mass function of Lenses

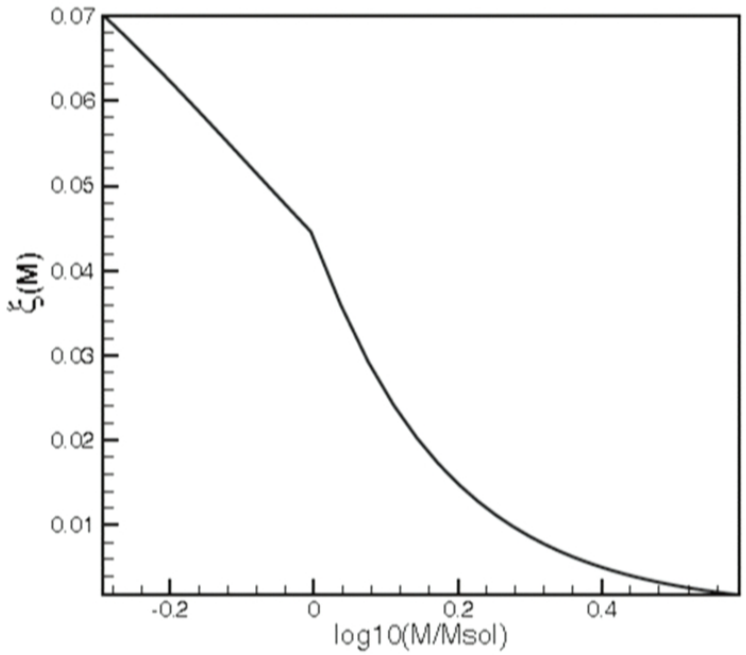

$$\xi(\log m) = 0.093 \times exp\left[-\frac{(\log m - \log 0.2)^2}{2 \times (0.55)^2}\right], \; m \leq m_\odot$$
$$= 0.041 m^{-1.35}, \; m > m_\odot.$$

Chabrier 2004

Analysis

Chi-square fitting to the distribution of

1- Einstein crossing time in four direction
2- optical depth along four direction
3- distribution of color
4- distribution of magnitude
5- number density of stars in the field

(parameters: angular orientation of bar, fraction of Hydrogen in the disk, abundance of the red giants in the bulge)

Result

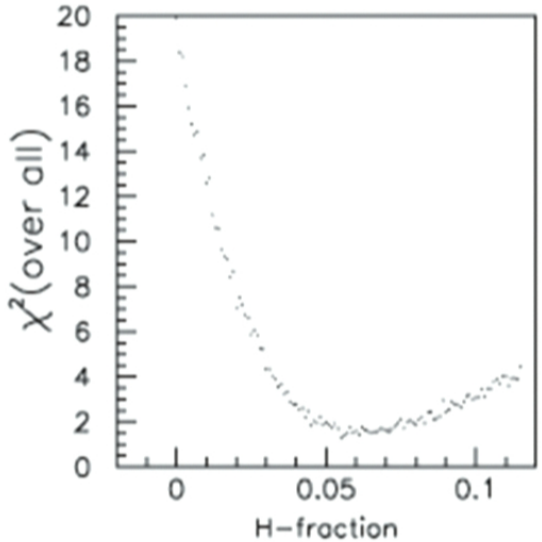

1- Disk is made of 6% Hydrogen, if we accept direct correlation of dusk density to the hydrogen density

2- Bar orientation is 45 degree with respect to the line of sight

Result

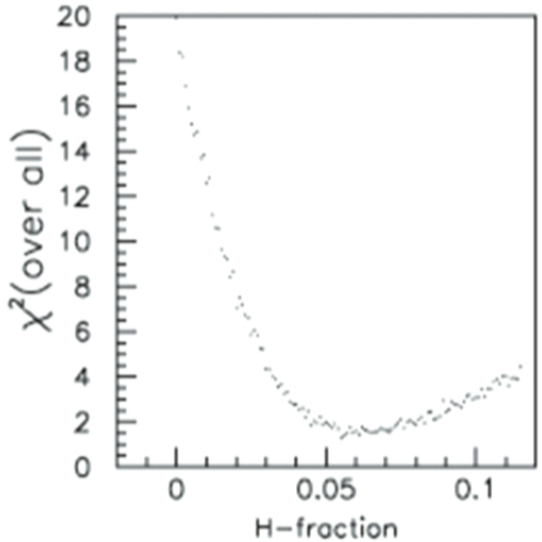

1- Disk is made of 6% Hydrogen, if we accept direct correlation of dusk density to the hydrogen density

2- Bar orientation is 45 degree with respect to the line of sight

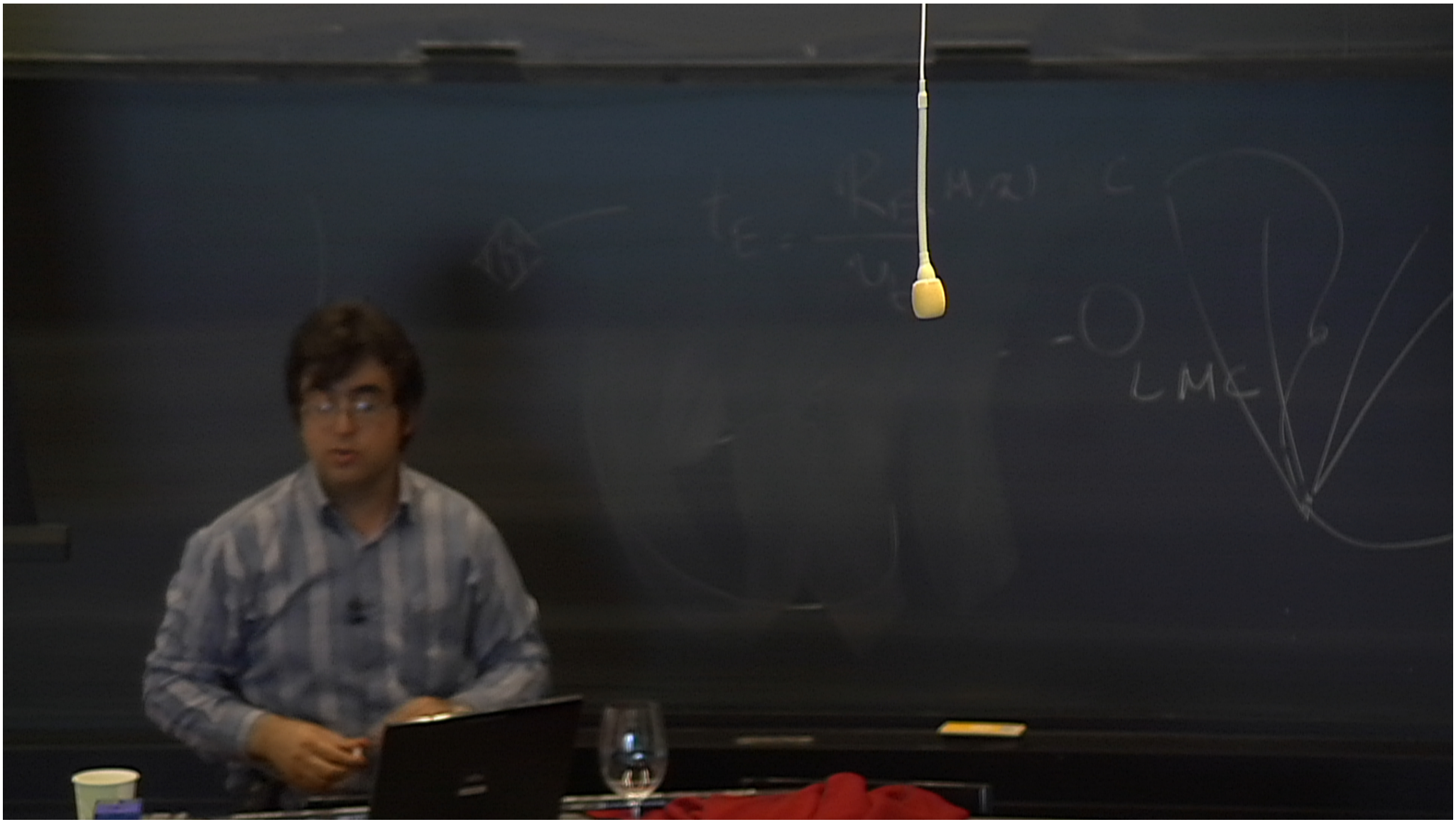
LMC

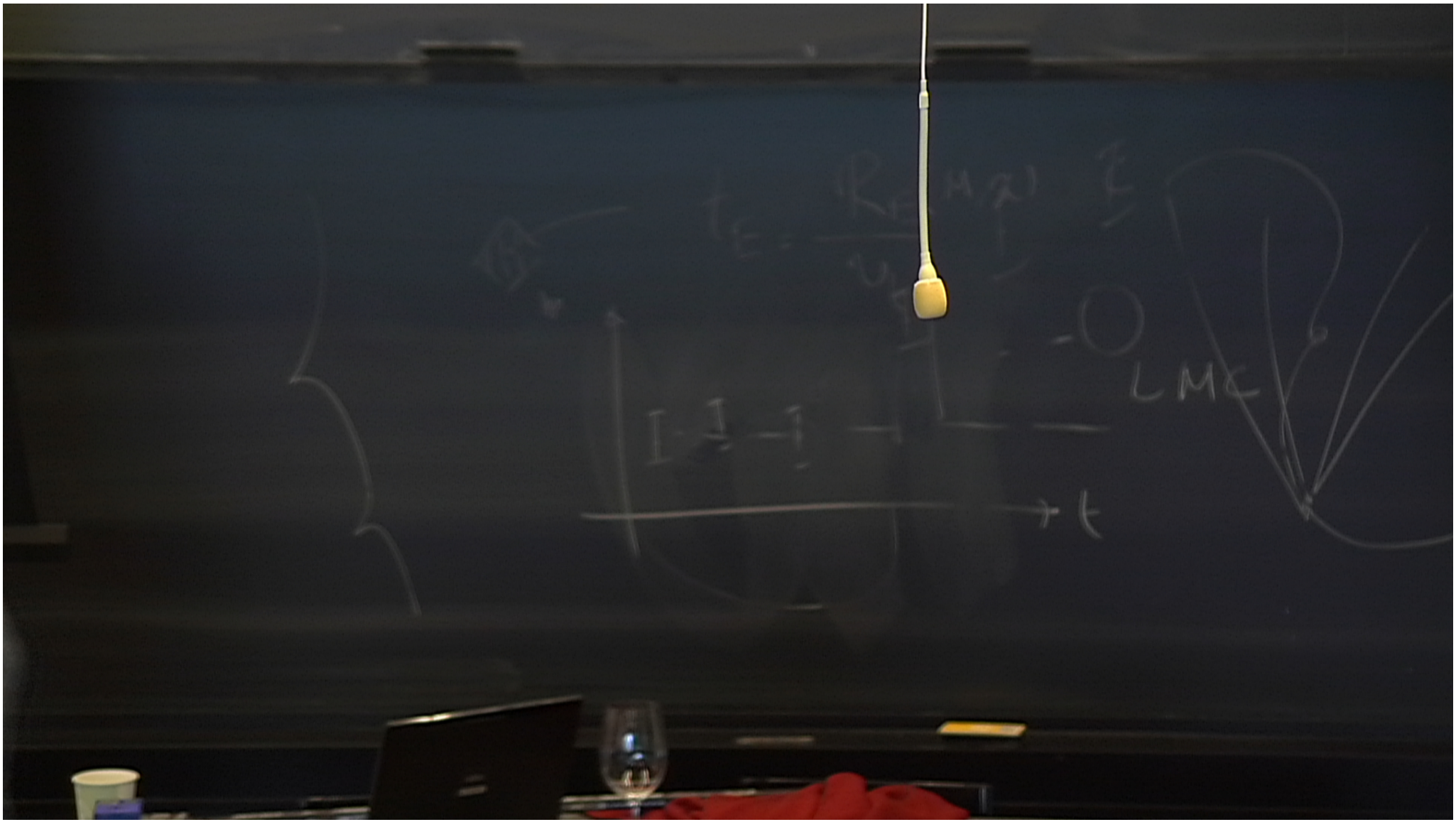
LMC

Observational Fields in the Spiral Arms

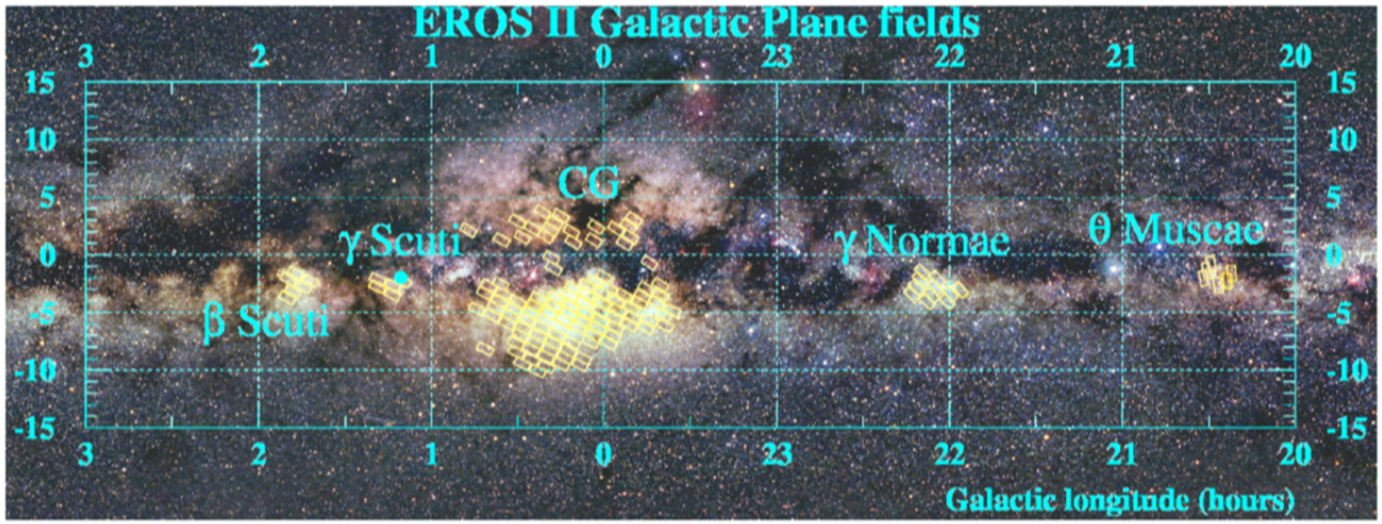

Rahal et al (EROS coll.) A&A (2009)